



ROBERT BOSCH CENTRE FOR CYBER-PHYSICAL SYSTEMS
3rd Floor, Entrepreneurship Building, Indian Institute of Science



Technical Report No: RBCCPS/TR/0003

Publication Date: February 2016

Title: Continuous Ambulatory Electrocardiography

Authors: Sagar Venkatesh Gubbi, Hiteshwar Rao, and Bharadwaj Amrutur

Continuous Ambulatory Electrocardiography

Sagar Venkatesh Gubbi¹

Hiteshwar Rao²

Bharadwaj Amrutur³

Abstract—Continuous ambulatory recording of the electrocardiogram could help in early detection of cardiovascular diseases, which could lower healthcare costs and improve prognosis. For such continuous ambulatory recordings, electrocardiographs that are discreet, comfortable to use, and have few electrodes are needed. Two-electrode electrocardiographs exhibit worse power line interference than three-electrode systems, but are desirable because they have one less electrode. We propose sizing the driven electrode of a three-electrode electrocardiograph to be much smaller than the two sensing electrodes. Our analysis shows that this can be done while keeping the power-line interference sufficiently small. The proposed “pseudo two-electrode” electrocardiograph, which has only two physical electrodes with an inconspicuous third electrical electrode, is evaluated by building it with discrete semiconductor components. Our experiments confirm that it is possible to considerably reduce the size of the driven electrode compared to the sensing electrodes.

I. INTRODUCTION

Societies are growing older because of increasing life expectancy, and the aging of societies is accompanied by rising healthcare costs[1], [2]. A significant fraction of the healthcare expenditure is for treating cardiovascular diseases[3]. Continuous ambulatory electrocardiography (ECG) can be used to detect heart diseases early on, which leads to better prognosis while simultaneously reducing health care costs[4]. Such continuous monitoring using wearable sensors has recently been made practical by the explosive growth of smartphones, which can serve as a convenient gateway device that talks to low-power wearable sensors and uploads the sensed data to a cloud database where the data can be analyzed (Fig. 1).

Continuous ambulatory electrocardiography differs from traditional in-hospital electrocardiographs in several ways. The electrocardiograph has to be discreet, comfortable to wear, and consume little power so that the battery size may be reduced[5], [6], [7]. To keep the sensor discreet, it is desirable to have as few electrodes as possible. Fortunately, even a one lead electrocardiograph can be used to detect many of the common cardiovascular diseases[8].

One of the issues in acquiring ECG signals is the presence of power-line interference. It manifests itself as a common

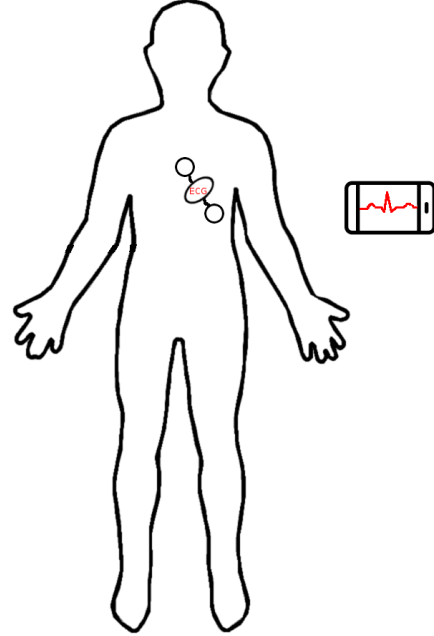


Fig. 1. Wearable Electrocardiograph transmitting data to a smartphone.

mode voltage as seen by the electrocardiograph and can be substantially higher than the ECG signal itself. Typically, ECG systems have at least 3 electrodes: two sensing electrodes, and one driven electrode, so as to minimize the power line interference. Using only two electrodes results in high interference, which would require elaborate circuitry to suppress[9], [10], [11], [12], [13]. We propose sizing the sensing and driven electrodes differently so that the electrocardiograph is kept discreet while still keeping the interference at bay.

The rest of this paper is organized as follows. In Section 2, we discuss the performance different electrode configurations. Experimental results from a system we built are described in Section 3. Finally, Section 4 concludes the paper.

II. PERFORMANCE OF INTERFACE CIRCUIT CONFIGURATIONS

A circuit model that captures power-line interference is used to analyze the performance of different ECG circuit topologies. This analysis gives an insight into how the electrode size may be reduced. An electrocardiograph that has an electrode with reduced size is built using discrete semiconductor components to validate our hypothesis.

Electrical power lines are ubiquitous, and because the human body is a good conductor of electricity compared

*This work was funded by the Robert Bosch Centre for Cyber-Physical Systems.

¹Sagar Venkatesh Gubbi is with the Department of Electrical and Communication Engineering, Indian Institute Of Science. sagar@ece.iisc.ernet.in

²Hiteshwar Rao is with the Robert Bosch Centre for Cyber-Physical Systems, Indian Institute Of Science. hitesh@cps.iisc.ernet.in

³Prof. Bharadwaj Amrutur is with the Department of Electrical and Communication Engineering / Robert Bosch Centre for Cyber-Physical Systems, Indian Institute Of Science. amrutur@ece.iisc.ernet.in

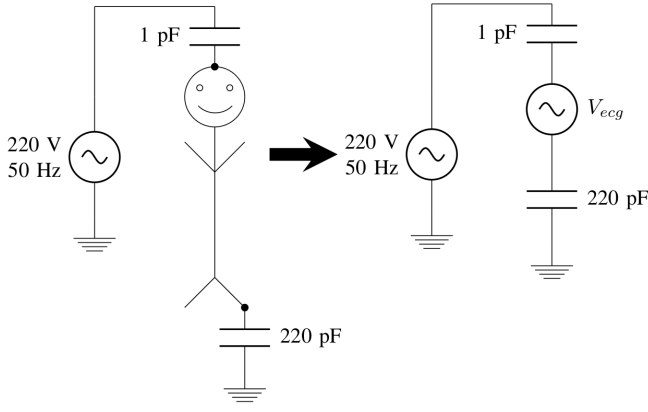


Fig. 2. Circuit model that captures power-line interference.

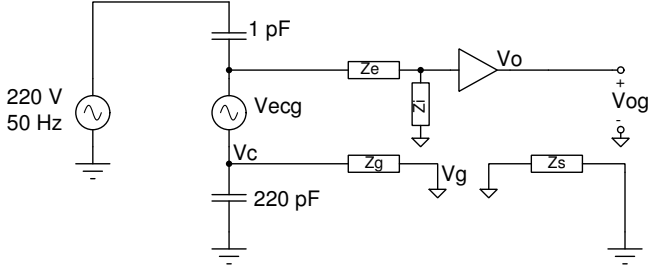


Fig. 3. Two-electrode single ended interface circuit.

to air, a small displacement current on the order of 100 nA flows from the power lines through the human body (Fig. 2) to the ground[14]. Along with the source of the ECG signal, this may be modeled as shown in Fig. 3. Z_e is the electrode-skin impedance (if there are two sensing electrodes, the impedances are Z_{e1} and Z_{e2} , with $\Delta Z_e = Z_{e2} - Z_{e1}$ and $Z_e = \frac{Z_{e1} + Z_{e2}}{2}$), Z_i is the input impedance of the front-end unity gain buffer, Z_g is the electrode-skin impedance of the low-impedance electrode, and Z_s is the isolation impedance between the circuit common and the earth ground. The goal is to faithfully measure V_{ecg} while suppressing the power-line interference. We consider the following four ECG circuit topologies to accomplish this goal.

A. Two-electrode Single Ended Interface Circuit

In this configuration (Fig. 3), one of the electrodes is connected to a high impedance unity gain amplifier. The second electrode is a low impedance electrode that is connected to the circuit common (V_g). Even if the two electrode impedances are matched (i.e., $Z_g = Z_e$), the output seen by the circuit contains substantial power-line interference (Table I).

B. Two-electrode Differential Interface Circuit

In the two-electrode differential configuration (Fig. 4), both the electrodes are connected to high impedance unity gain amplifiers, and the circuit common is left floating. The difference between the voltage sensed by the two electrodes is measured. Although interference vanishes when the electrode impedances are matched, the high common mode

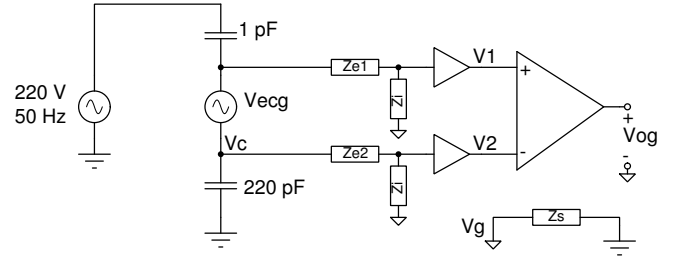


Fig. 4. Two-electrode differential interface Circuit.

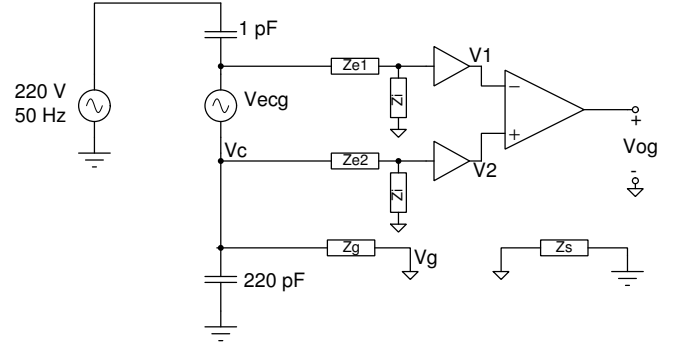


Fig. 5. Three-electrode interface circuit with passive dry ground.

impedance is unforgiving to static voltages that may develop on the body, and this can cause the amplifiers to saturate[14].

C. Three-electrode Interface circuit with passive ground

In the three-electrode interface circuit with passive ground, the two sensing electrodes are connected to high impedance unity gain amplifiers, and the third low-impedance electrode is connected to the circuit common (Fig. 5). The third low-impedance electrode significantly improves power-line interference rejection performance (Table I).

D. Three-electrode Interface circuit with driven right leg

In the three-electrode interface circuit with the driven right leg, the two sensing electrodes are connected to high impedance unity gain amplifiers as in the previous topology (Fig. 6). In contrast, the third low-impedance electrode, instead of being connected to the circuit common, is driven by an amplified and inverted version of the common mode signal. This is similar to the previous case with Z_g replaced by $Z'_g = \frac{Z_g}{A}$. Thus, with right leg drive, the electrode-skin impedance of the low-impedance electrode effectively gets divided by the right leg drive gain (A).

Table I compares the performance of the four interface circuit configurations discussed. For battery powered copper dry-contact electrodes of size 1 cm^2 , typical values are $Z_i = 100 \text{ M}\Omega$, $Z_e = Z_g = 10 \text{ M}\Omega$, $\Delta Z_e = 500 \text{ k}\Omega$, $Z_s = 1 \text{ G}\Omega$, $V_c \approx 1 \text{ V}$, 50 Hz , and for the right leg drive, $A = 100$. The first term in the third column represents the amplitude of the power-line interference, and the second term represents the amplitude of the ECG signal (assumed to be 1 mV).

First, we observe that even though two-electrode systems are desirable because they use one less electrode than

TABLE I
NOISE ESTIMATION PERFORMANCE

Circuit configuration	V_{og}	Typical values
2-electrode, single ended	$V_{og} = \left(\frac{Z_i}{Z_e + Z_i} \cdot \frac{Z_g}{Z_s + Z_g} \right) V_c + \left(\frac{Z_i}{Z_e + Z_i} \right) V_{ecg}$	$V_{og} = 10 \text{ mV}_{50\text{Hz}} + 1 \text{ mV}_{ecg}$
2-electrode, differential	$V_{og} = \left(\frac{\frac{\Delta Z_e}{Z_i}}{\left(1 + \frac{Z_e}{Z_i}\right)^2} \right) V_c + \left(\frac{Z_i}{Z_i + Z_{e1}} \right) V_{ecg}$	$V_{og} = 5 \text{ mV}_{50\text{Hz}} + 1 \text{ mV}_{ecg}$
3-electrode, passive ground	$V_{og} = \left(\frac{\frac{\Delta Z_e}{Z_i}}{\left(1 + \frac{Z_e}{Z_i}\right)^2} \cdot \frac{Z_g}{Z_s + Z_g} \right) V_c + \left(\frac{Z_i}{Z_i + Z_{e1}} \right) V_{ecg}$	$V_{og} = 50 \text{ }\mu\text{V}_{50\text{Hz}} + 1 \text{ mV}_{ecg}$
3-electrode, driven-right-leg	$V_{og} = \left(\frac{\frac{\Delta Z_e}{Z_i}}{\left(1 + \frac{Z_e}{Z_i}\right)^2} \cdot \frac{Z'_g}{Z_s + Z'_g} \right) V_c + \left(\frac{Z_i}{Z_i + Z_e} \right) V_{ecg}$	$V_{og} = 0.5 \text{ }\mu\text{V}_{50\text{Hz}} + 1 \text{ mV}_{ecg}$

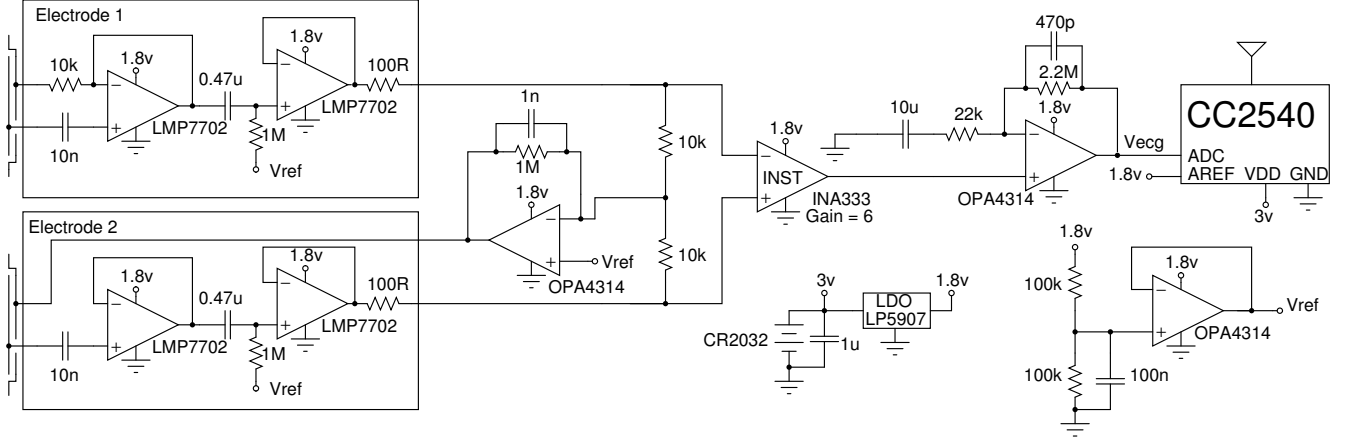


Fig. 7. Schematic of the proposed electrocardiograph.

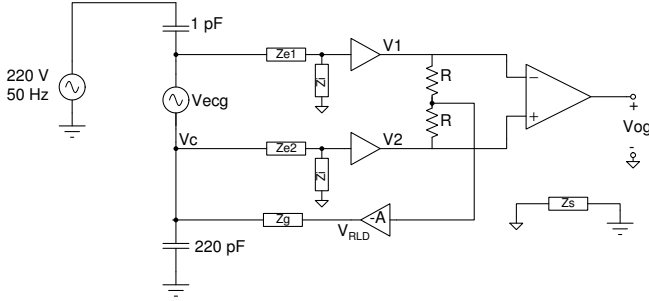


Fig. 6. Three-electrode interface circuit with driven right leg.

three-electrode electrocardiographs, they exhibit considerably worse power-line interference. Next, the performance of the driven-right-leg circuit exceeds the requirement of keeping the power-line interference below $10 \text{ }\mu\text{V}$ [15]. Finally, note that in three-electrode systems, it is only necessary that the two sensing electrodes be matched. Thus, the driven electrode may be sized considerably smaller than the sensing electrodes. In fact, it can be made so inconspicuous that the three-electrode electrocardiograph resembles a two-electrode system. We christen this “pseudo two-electrode” ECG.

III. EXPERIMENTAL RESULTS

The “pseudo two-electrode” electrocardiograph (Fig. 7) is powered by a CR2032 coin cell battery (Figs. 9). A front-end with very high input impedance is achieved by using a rail-to-rail input/output (RRIO) opamp in unity gain configuration with the positive opamp terminal left unbiased[13]. This is based on the idea that a small leakage current through the input protection diodes on the hi-z positive terminal will bias the op-amp. Even if the bias point is close to one of the rails because of mismatches, the ECG signal, with an amplitude of only a few mV at most, will have no trouble passing through the RRIO unity gain amplifier. The amplified signal is digitized by the 12-bit ADC in the CC2540[16] and then sent over the Bluetooth Low Energy (BLE) radio interface. An android application¹ that we have developed, “JeeYo Dill”, receives the raw samples and visualizes the electrocardiogram on the smartphone (Fig. 10).

The electrodes are fabricated on standard two layer FR-4 printed circuit boards (PCB) with diameter 18 mm (Fig. 8). The bottom copper plate serves as the electrode. In one of the electrodes, the outer ring (shield) on the back copper side is driven by the output of the front-end unity gain buffer. In the other electrode, the outer ring is connected to the right-

¹The software is available under an open source license at <https://github.com/s-gv/ecg>

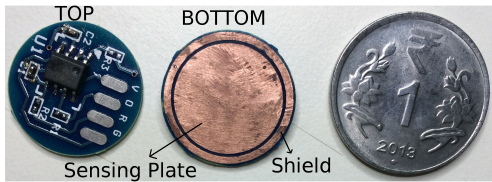


Fig. 8. Snapshot of the PCB electrodes. Two such circular physical electrodes were used.



Fig. 9. Snapshot of the electrocardiograph.

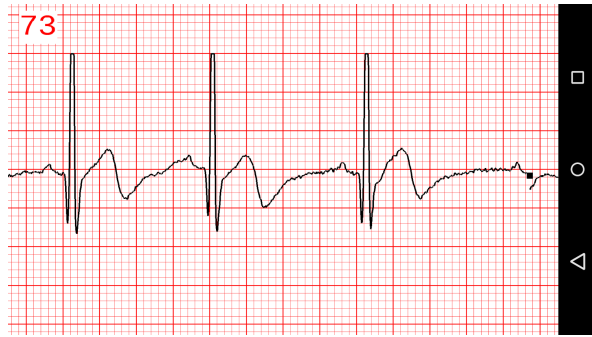


Fig. 10. A sample electrocardiogram recorded using the “pseudo two-electrode” electrocardiograph with an Android smartphone. The smallest square of the grid is 0.02 second \times 0.1 mV.

leg-drive amplifier, which serves as the driven electrode. Thus, there are only two physical electrodes, although three electrical electrodes are present. Figure 10 shows a sample electrocardiogram with the electrodes pressed across the heart. Power-line interference is not noticeable, and the recording is classified diagnostically usable by [17].

The analog front-end consumes 2.5 mW, and the CC2540 (including the ADC and the radio) consumes 32 mW. A CR2032 coin cell battery can power this system for about 16 hours. Although ECG front-ends with much lower power consumption are available[5], [6], the system power is dominated by the radio. So, to reduce system power consumption, one would have to process the electrocardiogram, extract information such as heart rate, and transmit only that.

IV. CONCLUSIONS

We showed by means of a circuit model that two-electrode electrocardiographs exhibit considerably worse power-line interference than three-electrode electrocardiographs. But, in the latter, the driven electrode can be sized to be much smaller than the sensing electrodes while still reaping the benefits of lowered power-line interference. This led to the development of a “pseudo two-electrode” electrocardiograph

that is electrically a three-electrode system, but has only two physical electrodes.

ACKNOWLEDGMENT

This work was funded by the Robert Bosch Centre for Cyber-Physical Systems, Indian Institute Of Science. The authors would like to thank Pushkar and Manikandan for fruitful discussions.

REFERENCES

- [1] J. A. Salomon, H. Wang, M. K. Freeman, T. Vos, A. D. Flaxman, A. D. Lopez, and C. J. Murray, “Healthy life expectancy for 187 countries, 1990–2010: A systematic analysis for the global burden disease study,” *The Lancet*, vol. 380, no. 9859, pp. 2144–2162, 2013.
- [2] P. A. Heidenreich, J. G. Trogon, O. A. Khavjou, J. Butler, K. Dracup, M. D. Ezekowitz, E. A. Finkelstein, Y. Hong, S. C. Johnston, A. Khera *et al.*, “Forecasting the future of cardiovascular disease in the united states: A policy statement from the american heart association,” *Circulation*, vol. 123, no. 8, pp. 933–944, 2011.
- [3] A. S. Go, D. Mozaffarian, V. L. Roger, E. J. Benjamin, J. D. Berry, M. J. Blaha, S. Dai, E. S. Ford, C. S. Fox, S. Franco *et al.*, “Heart disease and stroke statistics–2014 update: A report from the american heart association,” *Circulation*, vol. 129, no. 3, p. 28, 2014.
- [4] S. Stern and D. Tzivoni, “Early detection of silent ischaemic heart disease by 24-hour electrocardiographic monitoring of active subjects,” *British heart journal*, vol. 36, no. 5, p. 481, 1974.
- [5] O. T. Inan and G. T. Kovacs, “An 11 μ w, two-electrode transimpedance biosignal amplifier with active current feedback stabilization,” *IEEE Transactions on Biomedical Circuits and Systems*, vol. 4, no. 2, pp. 93–100, 2010.
- [6] L. Fay, V. Misra, and R. Sarpeshkar, “A micropower electrocardiogram amplifier,” *IEEE Transactions on Biomedical Circuits and Systems*, vol. 3, no. 5, pp. 312–320, 2009.
- [7] C. R. Merritt, H. T. Nagle, and E. Grant, “Fabric-based active electrode design and fabrication for health monitoring clothing,” *IEEE Transactions on Information Technology in Biomedicine*, vol. 13, no. 2, pp. 274–280, 2009.
- [8] T. Dawber, W. Kannel, D. Love, and R. Streper, “The electrocardiogram in heart disease detection: A comparison of the multiple and single lead procedures,” *Circulation*, vol. 5, no. 4, pp. 559–566, 1952.
- [9] I.-D. Hwang and J. G. Webster, “Direct interference canceling for two-electrode biopotential amplifier,” *IEEE Transactions on Biomedical Engineering*, vol. 55, no. 11, pp. 2620–2627, 2008.
- [10] D. Dobrev and I. Daskalov, “Two-electrode biopotential amplifier with current-driven inputs,” *Medical and Biological Engineering and Computing*, vol. 40, no. 1, pp. 122–127, 2002.
- [11] D. Dobrev, “Two-electrode low supply voltage electrocardiogram signal amplifier,” *Medical and Biological Engineering and Computing*, vol. 42, no. 2, pp. 272–276, 2004.
- [12] D. P. Dobrev, T. Neycheva, and N. Mudrov, “Bootstrapped two-electrode biosignal amplifier,” *Medical and biological engineering and computing*, vol. 46, no. 6, pp. 613–619, 2008.
- [13] Y. M. Chi, P. Ng, E. Kang, J. Kang, J. Fang, and G. Cauwenberghs, “Wireless non-contact cardiac and neural monitoring,” in *Wireless Health*. ACM, 2010, pp. 15–23.
- [14] N. V. Thakor and J. G. Webster, “Ground-free ECG recording with two electrodes,” *IEEE Transactions on Biomedical Engineering*, no. 12, pp. 699–704, 1980.
- [15] J. J. Bailey, A. S. Berson, A. Garson Jr, L. G. Horan, P. W. Macfarlane, D. W. Mortara, and C. Zywiets, “Recommendations for standardization and specifications in automated electrocardiography: bandwidth and digital signal processing. a report for health professionals by an ad-hoc writing group of the committee on electrocardiography and cardiac electrophysiology of the council on clinical cardiology, american heart association,” *Circulation*, vol. 81, no. 2, p. 730, 1990.
- [16] “CC2540 2.4 GHz bluetooth low energy system-on-chip,” *Product specification*, Texas Instruments, 2014. [Online]. Available: <http://www.ti.com/product/cc2540>
- [17] D. Hayn, B. Jammerbund, and G. Schreier, “ECG quality assessment for patient empowerment in mHealth applications,” in *Computing in Cardiology*, 2011. IEEE, 2011, pp. 353–356.